Reflectance, luminescence and Raman experiments on Eu^{3+} crystal field transitions in Eu_2BaZnO_5

1998 J. Phys.: Condens. Matter 10 8983

(http://iopscience.iop.org/0953-8984/10/40/006)

J. Phys.: Condens. Matter **10** (1998) 8983–8998. Printed in the UK PII: S0953-8984(98)91701-5

Reflectance, luminescence and Raman experiments on Eu^{3+} crystal field transitions in Eu_2BaZnO_5

S Taboada†, A de Andrés† and J E Muñoz-Santiuste‡

† Instituto de Ciencia de Materiales de Madrid, Consejo Superior de Investigaciones Científicas, Campus de Cantoblanco E-28049, Madrid, Spain

‡ Escuela Politécnica Superior, Universidad Carlos III de Madrid, Avenida del Mediterráneo 20, Leganés E-28913, Madrid, Spain

Received 16 February 1998, in final form 3 August 1998

Abstract. Three spectroscopic techniques have been combined to resolve the complex problem of Eu^{3+} crystal field levels in Eu_2BaZnO_5. Eu^{3+} luminescence has been investigated in the off-resonance condition for several excitation energies as a function of temperature. Raman phonons and several Raman crystal field transitions are obtained. From reflectance experiments (between 1.25 and 3.7 eV), ^5D multiplet levels are determined. The schemes of the lowest electronic levels of both Eu^{3+} sites have been established combining data from these three spectroscopies which show a good agreement with the calculated values. Crystal field parameters are obtained in an approximation to a C_{2v} local symmetry. The high value of fourth-rank parameters indicates a partial covalent character of Eu–O bonds. The obtained spin–orbit coupling value, $\zeta = 1280(70)$ cm^{-1}, is similar to those in other europium oxides. The variation of the Raman crystal field transition intensity with temperature presents an unexpected deviation with respect to the ground state population, specially pronounced in the low temperature range. The peaks corresponding to the three highest levels of the $^7F_2$ multiplet are anomalous probably due to some hybridization with the nearest oxygen levels. The relative intensity of luminescence peaks associated with transitions from $^5D_0$ and $^5D_1$ levels vary versus temperature as a function of the probability of the non-radiative decay. We propose a mechanism that can explain the observation of anti-Stokes luminescence even at low temperatures.

1. Introduction

R_2BaMO_5 (R = rare earth and M = transition metal) oxides can be obtained in four crystalline structures, depending on the size of the rare earth and the transition metal involved. The metal occupies different sites in each phase (octahedral, square-based pyramidal, square-plane or tetrahedral polyhedrons), while the lanthanide environment is only slightly different in the four structures. In particular, Eu_2BaZnO_5 belongs to the *Pnma* space group, which is the so called 'green phase' frequently present in cuprates as an impurity of the superconducting phase ($YBa_2Cu_3O_{6+x}$). This structure is orthorhombic with four formulae per primitive cell, and is characterized by isolated oxygen square-based pyramids around the Zn ion [1, 2]. Eu^{3+} ions occupy two different sevenfold oxygen coordinated sites with the same symmetry (C_s) but slightly different Eu–O distances.

Crystal field (CF) splitting of Eu^{3+} 4f levels has been widely studied when Eu dopes different crystalline matrices (see for example [3–8]). A luminescence study is reported on the Eu^{3+}:Y_2BaZnO_5 compound [5], whose matrix crystallizes in the *Pnma* structure. The authors use a dye laser in order to achieve the excitation at one resonance energy for each

0953-8984/98/408983+16$19.50

Eu ion. The CF parameters for both Eu sites are found to be quite different, in opposition to what is obtained in our work.

Optical spectroscopies have been less used when Eu is a constitutional ion of the compound. In addition to infrared and Raman phonons, photoluminescence has been studied in the Eu_2BaCoO_5 compound (*Immm* structure) [9]. This oxide presents an interrelation between infrared phonons and interband electronic transitions. Luminescence excitation and emission processes are deduced.

Crystal field transitions of other rare earth ions have been studied in related compounds (see for example [10, 11]). Nd^{3+} CF transitions in Nd_2BaZnO_5 ($I4/mcm$ structure) were studied by Raman scattering and Fourier-transform infrared reflectivity as a function of the temperature [11].

The magnetic study performed by Goya *et al* [12] reveals that the Eu_2BaZnO_5 compound is a Van Vleck paramagnet, with a constant value of the susceptibility for the lower temperature range and a decreasing value when $T \geqslant 100$ K. The explanation given by the authors of such behaviour is that the ground state is non-magnetic, but the ^7F_J excited states are close enough to have a non-negligible population at room temperature, giving a Curie-like behaviour in the high temperature region. At low temperature ($T \leqslant 100$ K), only the non-magnetic ground state is populated and the susceptibility becomes temperature independent.

In recent years there has been an increasing interest in the application of Raman scattering experiments to the study of the crystal field levels of rare earth ions in oxides. In the present work, we have combined this technique with luminescence and reflectance spectroscopies (in the visible range) in order to study the splitting of the CF levels of the Eu^{3+} ion. These techniques are not usually combined in this kind of study, but we will show that this is a very useful strategy in the solution of a complicated problem such as the present case. On the other hand, the study of the luminescence in the off-resonance condition provides surprising results such as anti-Stokes luminescence or a drastic change of the luminescence peak relative intensity as a function of temperature. To elucidate the mechanisms which can explain these results is another of the aims of this paper.

2. Experimental details

The Eu_2BaZnO_5 compound was prepared as a polycrystalline sample mixing stoichiometric amounts of the high-purity oxides Eu_2O_3 (99.999%), ZnO (99.99%) and $BaCO_3$ (99.999%). The homogenized mixture was heated in air at 950 °C for 12 hours; then it was reground and reheated at 1050 °C for another 12 hours. Once the powder was pressed into a pellet, a third thermal treatment at 1000 °C was achieved in order to obtain a compacted ceramic. The x-ray diffraction data show that the sample is single phase and presents the *Pnma* structure, which means that at least about 99% of the sample has this structure.

Two Raman scattering experimental set-ups were used to perform Raman and luminescence experiments: on one hand, an *X–Y* Dilor multichannel spectrometer was used in the triple subtractive configuration with a photodiode array as detector. In this case, the excitation source was a Coherent Ar^+ laser, with less than 10 mW on the sample to avoid surface damage due to sample heating. The luminescence of the sample was excited with the 488 nm and 514.5 nm lines of this laser. The available spectral range was 13 000–21 000 cm^{-1}. The spectra were recorded between 300 K and 35 K in backscattering geometry using a continuous flow Oxford Instrument cryostat, the sample being always in helium atmosphere. The spectral resolution varies between 3.7 and 4.1 cm^{-1}. Plasma lines were eliminated with a monochromating system consisting in four prisms and a pinhole; the lines nearest to the excitation energy are sometimes observed because of the characteristics of this kind of systems.

The other Raman set-up is a Renishaw 2000 spectrometer which combines Supernotch filters and a grating. This set-up includes an He–Ne ion laser (633 nm) as excitation source. In this case, the spectra were recorded between RT and 170 K in another continuous flow Oxford Instrument cryostat. The spectral range covered was 14 000–18 000 cm^{-1}. A microscope was employed to focus and collect the light, and, therefore, backscattering geometry was again used. The resolution of this set-up is around 4 cm^{-1} in this spectral range.

As the sample is a polycrystalline pellet, reflectance experiments, instead of absorption ones, were performed. These measurements were carried out on a HR-460 Jobin Yvon monochromator with a CCD detector and a tungsten lamp in the UV to red region. The spectra were recorded at RT between 1.25 and 3.7 eV (10 000–30 000 cm^{-1}), the resolution in this range varying between 6 and 13 cm^{-1}.

All spectra have been corrected by the spectral response of the different experimental set-ups, very dependent on the frequency of the detected light.

3. Optical phonons

The *Pnma* structure is orthorhombic with the D_{2h} point group and four formulae in the primitive cell. This leads to a large primitive cell with 36 ions and 108 normal modes of vibration. The factor group analysis of this structure shows that, out of the 108 normal modes, 54 even modes are Raman active and 35 odd modes are infrared active [13]. The irreducible representations of the Raman active modes at $\boldsymbol{k} = \mathbf{0}$ are:

$$16\ A_g + 16\ B_{1g} + 11\ B_{2g} + 11\ B_{3g}.$$

In this low symmetric structure, there are two sites for the rare earth ions (Eu(1), Eu(2)), one for Ba, one for Zn and three for the oxygen (O(1), O(2), O(3)); all of them can contribute to the Raman modes.

The large number of Raman active modes gives rise to the complicated spectrum of figure 1. With the exception of the plasma line observed at 39 cm^{-1}, all the other peaks

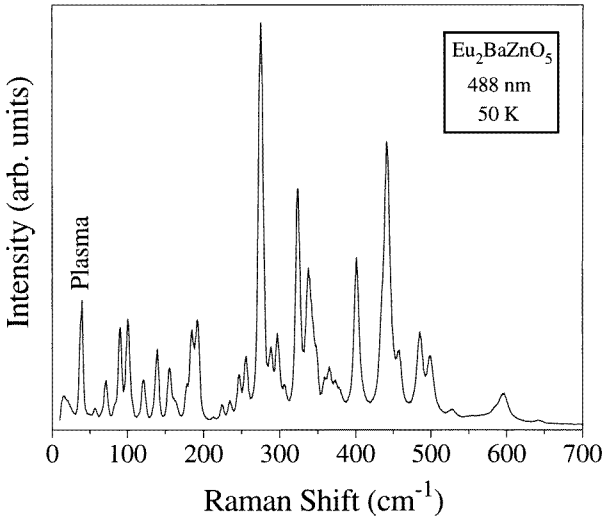

Figure 1. Raman phonons of the Eu_2BaZnO_5 compound at 50 K using 488 nm as excitation energy.

are 35 out of the 54 allowed Raman modes. Note that the most energetic phonon has a frequency of 595 cm^{-1}. A study of the optical phonons of the isomorphic Tm_2BaNiO_5 and related compounds is described in [13], where the highest frequency phonon found around 616 cm^{-1} is tentatively assigned to the stretching mode of the in-plane oxygen ions.

4. Eu^{3+} crystal field level scheme

Eu^{3+} ions in Eu_2BaZnO_5 occupy the centre of two trigonal prisms of seven oxygen ions, with C_s local symmetry. Both environments and their respective distances are shown in figure 2 and table 1. The polyhedrons representing both sites are basically identical except for the rotation of 90° with respect to the *y* axis. Both share a triangular face (shown in the figure), having the O(3) and two O(2) in common. The only symmetry element is

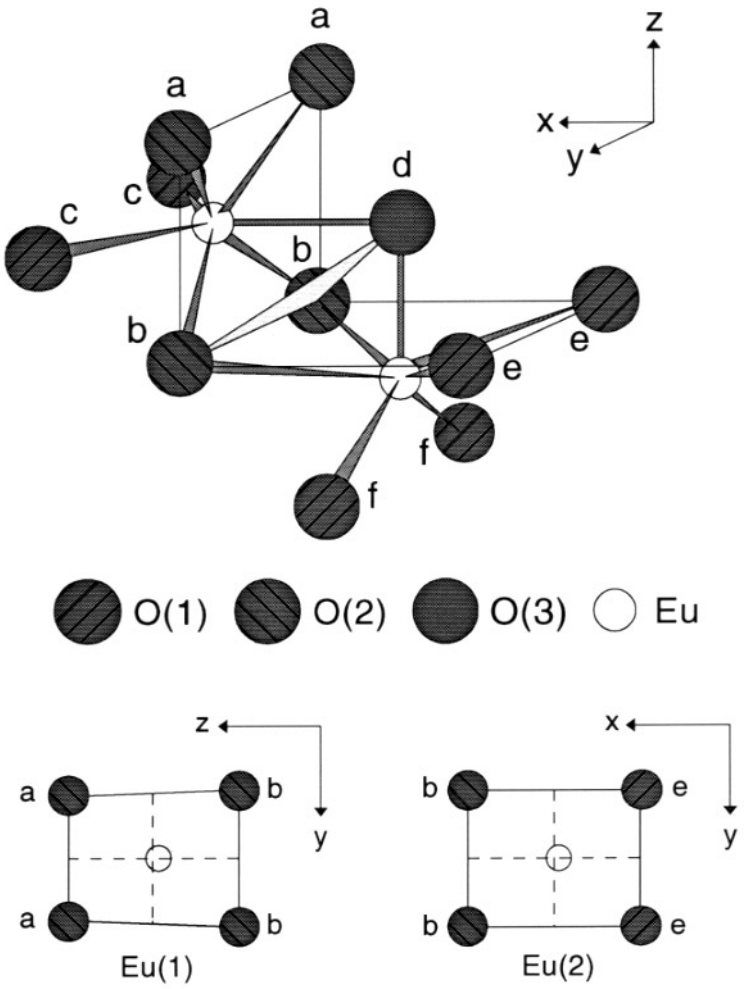

Figure 2. Environments of both Eu^{3+} sites in Eu_2BaZnO_5. Triangular face shared by both polyhedrons is shown. In the bottom part, the four in-plane oxygen ions around both Eu ions are shown indicating a more regular site for the Eu(2) ion.

Table 1. Eu–O interatomic distances in the Eu_2BaZnO_5 compound.

Eu(1)			Eu(2)		
2×	a	2.38 Å	2.35 Å	e	2×
2×	b	2.40 Å	2.43 Å	b	2×
2×	c	2.36 Å	2.42 Å	f	2×
1×	d	2.43 Å	2.37 Å	d	1×
average		2.387 Å	2.396 Å	average	
		Eu(1)–Eu(2)	3.38 Å		

the mirror plane which contains the Eu–O(3) bond and is perpendicular to the four oxygen planar square (which are not on any symmetry element). The values shown in table 1 reveal a maximum bond distance difference of 0.06 Å and an average distance really alike in both environments. 4f electrons of rare earth ions are much less sensitive to their environment than 3d electrons in transition metal ions because 4f wavefunctions are localized closer to the nuclei and screened by outer electrons. Therefore variations in mean Eu–O distances of 0.01 Å are not expected to produce large changes in the energy of the CF levels.

The scheme of the electronic levels of the free ion Eu^{3+} consists of six ^7F_J terms well separated from the ^5D excited states [14]. Above the $^5D_3$ multiplet the terms are heavily overlapped. The observed transitions to or from the $^5D_0$ singlet are enough to obtain the levels of the ^7F_J multiplets. These levels are the ones used to calculate the crystal field parameters that describe the Eu^{3+} environments. Because of the Eu C_s local symmetry, the degeneracy of the free-ion levels is completely lifted, so that $(2J + 1)$ levels are expected for each J term.

In order to determine the energy of these levels, three spectroscopic techniques have been used: reflectance, Raman and luminescence. Figure 3 shows the reflectance spectrum of the Eu_2BaZnO_5 compound between 16 000 and 28 000 cm^{-1}, recorded at room temperature. No peaks were detected below 16 000 cm^{-1}, down to 10 000 cm^{-1}. At RT, the lower multiplets are thermally populated and transitions from them are observed: the transitions from ^7F_J $(J = 0, 1, 2)$ to ^5D_J $(J = 0, 1, 2)$ multiplets are identified in figures 3(a), 3(b) and 3(c) respectively. The mixture of the multiplets above 24 000 cm^{-1} gives rise to numerous close peaks (figure 3(d)) which makes their identification very difficult. The double peak in figure 3(a) corresponds to $^7F_0 \rightarrow {}^5D_0$ transition in both Eu environments.

It is sometimes possible to detect Raman processes related to the rare earth electronic transitions from the ground state to the closer multiplets. This is very convenient because it allows the direct determination of the lowest multiplets and/or the splitting of the ground state multiplet as it is equivalent to an absorption process in the FIR range (between tenths and thousands of cm^{-1}) but detecting visible light. A transition between two electronic levels is Raman allowed if the direct product of their representations contains some of the irreducible representations of the Raman-active phonons. In the notation of [15], the possible symmetries of all split ^7F_J levels for a C_s site are Γ_1 and Γ_2. The direct product of two of these levels is $\Gamma_i \otimes \Gamma_j = A'$ or A'', which correspond to an even mode for the D_{2h} point group ($A' \leftrightarrow A_g$ or B_{2g}; $A'' \leftrightarrow B_{1g}$ or B_{3g}). Therefore, all possible transitions, intra- and intermultiplets, are Raman allowed.

The Raman crystal field (RCF) transitions recorded at three different excitation energies and from RT to 35 K are collected in figure 4. In addition to phonons (shown as reference), these spectra represent transitions from the ground state to the $^7F_2$, $^7F_3$ and $^7F_4$ multiplets (labelled in the figure), and, therefore, allow the direct determination of the energy values

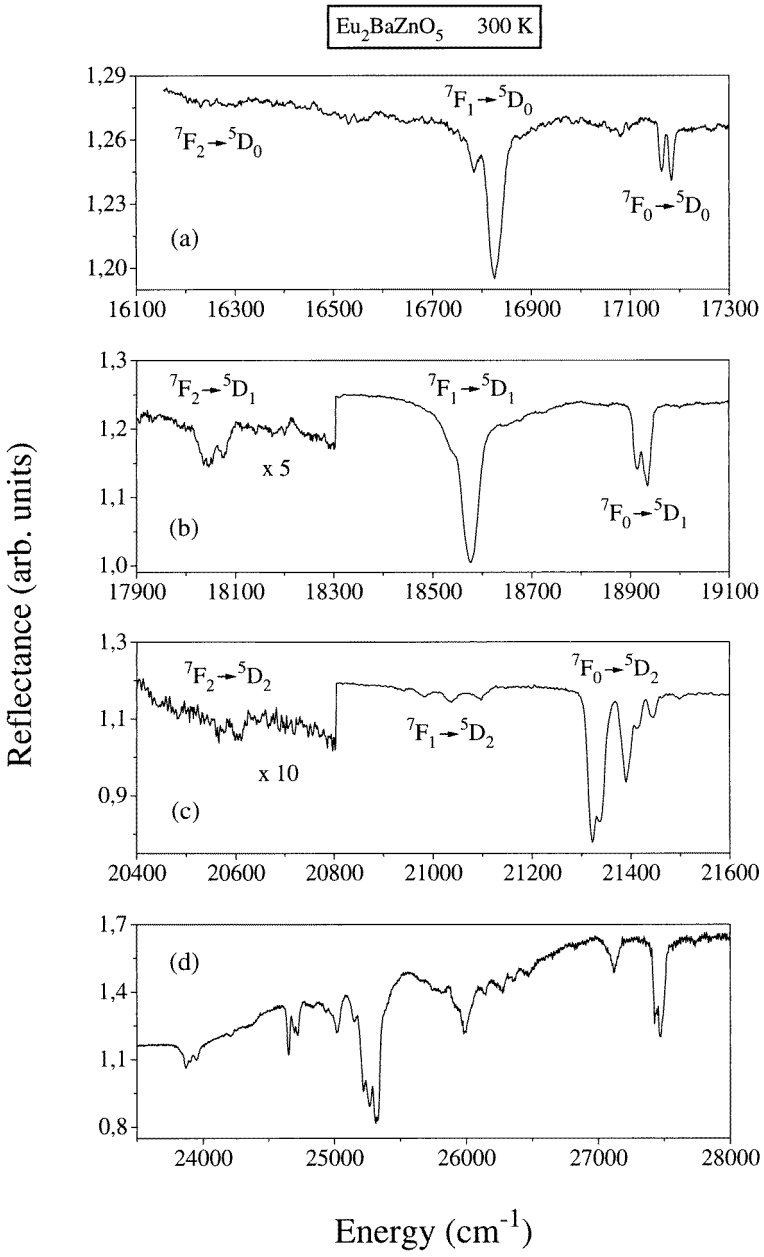

Figure 3. Reflectance spectrum of Eu_2BaZnO_5 at RT. Transitions from ^7F_J ($J = 0, 1, 2$) to ^5D_J ($J = 0, 1, 2$) multiplets are labelled in figures 3(a), 3(b) and 3(c) respectively.

of these levels. The RCF transitions to the $^7F_1$ triplet are expected in the 350–380 cm^{-1} range. Nevertheless we do not observe any relative intensity change between peaks in the 0–700 cm^{-1} range when temperature is lowered, so we cannot relate any of the observed peaks to $^7F_1$ RCF transitions.

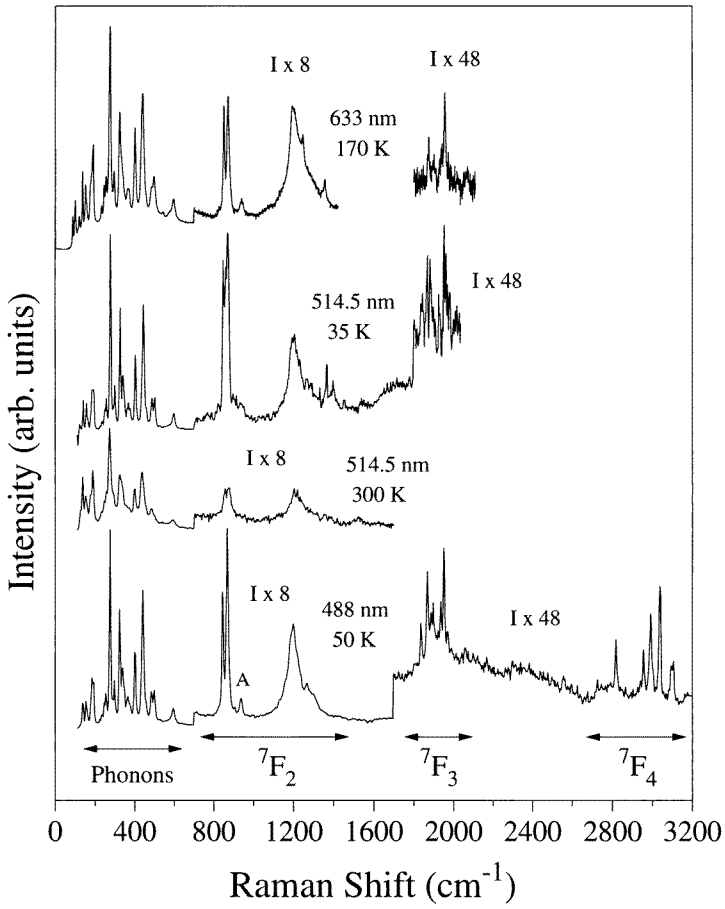

Figure 4. Raman crystal field transitions at high and low temperature, measured at three different wavelengths. The intensity of $^7F_2$, $^7F_3$ and $^7F_4$ regions has been enlarged for clarity. The transitions not shown in the figure are overlapped by the luminescence. Phonons are shown as a reference. The peak labelled A is explained in the text.

The third spectroscopy employed is luminescence, but in order to compare luminescence and RCF transitions, some insight into both processes is needed: luminescence occurs when an excited electron radiatively decays from one electronic level to another, and, therefore, the energy of the observed photon is independent of the excitation energy. In contrast, RCF transitions lie in the transference of part of the incident energy to achieve the excitation from one electronic level to another. The detected photon energy is $\hbar\omega_0 \mp (E_i - E_j)$. As a consequence, the energies at which these transitions are observed depend on the excitation wavelength and appear always at the same Raman shift (as phonons).

Some of the luminescence measurements at room temperature and low temperature are shown in figure 5. These spectra are normalized by the phonon areas, which are corrected by the thermal factor, and correspond to Eu^{3+} luminescence excited with 514.5 nm (continuous lines) and 488 nm (dotted lines). Combining these results with reflectance (figure 3) and Raman (figure 4) spectra, the $^5D_0 \rightarrow {}^7F_J$ ($J = 0$ to 2) transitions can be identified (marked

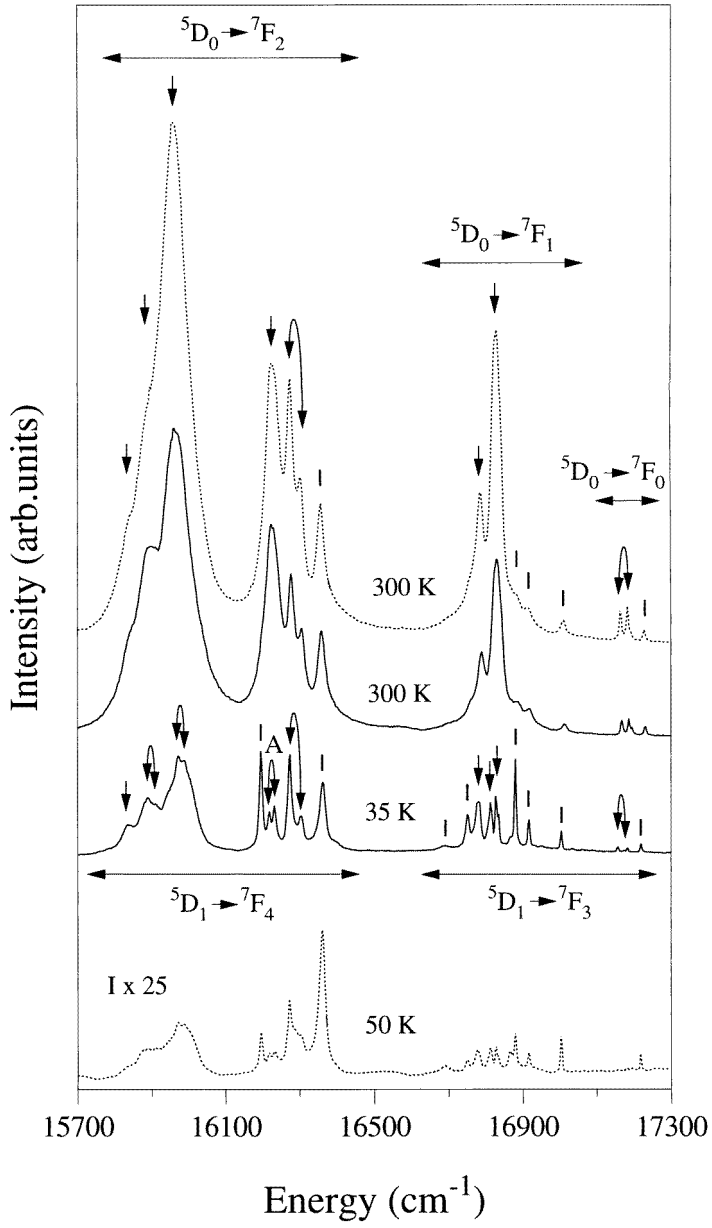

Figure 5. $^5D_{0,1} \rightarrow {}^7F_J$ ($J = 0, 1, 2, 3, 4$) luminescence of Eu_2BaZnO_5 from RT to 35 K under 514.5 nm (continuous line) and 488 nm (dashed one) excitation energies. Arrows indicate transitions from $^5D_0$ level and segments from $^5D_1$. Curved arrows denote the same transition for both Eu sites, starting at the $^5D_0$ singlet.

with arrows in figure 5; curved arrows indicate the same transition in both Eu environments). All the other peaks represent transitions from the $^5D_1$ triplet to ^7F_J levels (marked with segments). When the temperature is lowered, the peaks become narrower and split (marked, together with those at RT, in the spectrum at 35 K).

The second lower $^7F_2$ level (939 cm^{-1}) detected as one peak in the RCF spectrum is observed as a double peak in luminescence (marked with letter A in figures 4 and 5). This can be explained assuming this level at the same energy difference from the ground state in both Eu environments, but at different energy separation from the $^5D_0$ singlet in each Eu environment.

The experimental and calculated Eu^{3+} energy levels up to 22 000 cm^{-1} are summarized in table 2. Columns 1 and 2 indicate the two sites for the Eu^{3+} ions. As both sites are indistinguishable for us, columns 1 and 2 do not necessarily indicate Eu(1) and Eu(2) of figure 2, respectively. The experimental values are obtained from reflectance (R), luminescence (L) and Raman (the last column) spectroscopies. At RT, luminescence peaks are relatively broad and the resolution of the same level in both environments is, in general, not possible. When temperature decreases, there is a narrowing of the peaks and both sets of levels can be established in most cases. The origin is taken at the ground state of each europium ion and, therefore, energy levels are referred to their corresponding $^7F_0$ level. As it can be observed in the table, the maximum energy difference between both Eu sets is 20 cm^{-1}, which is the difference between $^5D_0$ levels. A shift of the levels ($\sim$10 cm^{-1}) towards higher energies is observed from low to high temperature, the splitting of each multiplet being approximately the same.

The line assignment of the $^5D_{0,1} \rightarrow {}^7F_{0-4}$ transitions to both Eu^{3+} sites have been done in the following way: the lower frequency peak of the $^5D_0 \rightarrow {}^7F_0$ observed doublet has been assigned to Eu(1) and the higher one to Eu(2). In general, the same rule is applied to all other transitions. These experimentally determined set of levels were used to obtain the CF parameters and their corresponding calculated values. The best accordance between experimental and calculated levels for both europium sites corresponds to the assignment shown in table 2.

5. Crystal field parameters

Semiempirical energy level positions obtained from a least squares fit of low temperature experimental values are shown in table 2, together with the irreducible representations of the levels in the C_{2v} point group. The character is obtained according to the symmetry of the major component of eigenvectors following the assignation given in [16]. The agreement between experimental and calculated values is good except for the three highest $^7F_2$ levels (marked with an asterisk). Crystal field parameters used to calculate the energy levels have been obtained as follows.

The total Hamiltonian that describes Eu^{3+} optical transitions in solids includes the free ion Hamiltonian and the crystal field (CF) perturbation. The free ion Hamiltonian is described by a set of electrostatic repulsions, spin–orbit interaction and many body interactions that can be written as a sum, factorized in products, of a large number of parameters (19 for the Eu^{3+} ion). To determine such a large number of parameters it is necessary to know the energies of a large number of $|LS\rangle$ states. Nevertheless, optical measurements usually allow the experimental determination of lowest multiplets (mainly ^7F and ^5D). So, the number of free ion parameters must be restricted in some way.

The one electron CF Hamiltonian is traditionally described by a sum of the products of the real, B_q^k, and imaginary parts, S_q^k, of crystal field parameters and the renormalized spherical tensors, C_q^k, in the form:

$$H_{CF} = \sum_{k=0}^{6} \sum_{q \geqslant -k}^{k} [B_q^k (C_q^k + (-1)^q C_{-q}^k) + \mathrm{i} S_Q^k (C_q^k - (-1)^q C_{-q}^k)].$$

Table 2. Experimental and calculated energy values (in C_{2v} approximation) of the lowest multiplets of Eu^{3+} ions in Eu_2BaZnO_5. 1 and 2 denote both europium sites. R = reflectance and L = luminescence. ∗ = anomalous peaks.

	Energy levels (cm^{-1})									
	RT			LT			Calculated			
Multiplet (number of levels)	1	2		1	2		1	2		Raman (50K)
$^5D_2$	21 492	21 501	R				21 482	21 490		
(5)	21 446	21 449	R/L				21 465	21 472		
	21 417	21 420	R/L				21 441	21 448		
	21 390	21 396	R/L				21 436	21 445		
	21 324	21 341	R/L				21 311	21 320		
$^5D_1$	18 934	18 942	R/L	18 922	18 929	L	18 917	18 925		
(3)	18 923	18 927	L	—	18 915	L	18 908	18 910		
	18 912	18 916	R/L	18 900	18 903	L	18 904	18 908		
$^5D_0$	17 164	17 183	R/L	17 156	17 173	L	17 156	17 173	A_1	
$^7F_4$	3129	3134	L	3126	3129	L	3123	3129	A_1	3125
(9)	3082	3090	L	3075	3084	L	3077	3086	B_1	3095–3105
	3051	3050	L	3056	3057	L	3054	3055	B_2	3056
	—	3025	L	3025	3038	L	3031	3038	A_2	3037
	2999	2988	L	2991	2977	L	2988	2980	A_1	3001–2991
	2951	2955	L	2942	2943	L	2940	2939	A_1	2940–2955
	2836	2833	L	2824	2820	L	2826	2818	B_2	2827–2818
	2726	2733	L	2711	2716	L	2711	2715	B_1	2726
	2640	2635	L	2615	2620	L	2612	2617	A_2	2625
$^7F_3$	—	1992	L	—	1974	L	1977	1973	B_2	1970
(7)	—	1974	L	1957	1961	L	1956	1960	B_1	1951
	—	1954	L	1937	1943	L	1936	1940	A_2	1937
	—	1898	L	1881	1889	L	1883	1885	B_2	1887–1897
	—	1881	L	1867	1871	L	1869	1868	B_1	1869
	—	1853	L	1854	1835	L	1850	1846	B_1	1837
	—	—		1766	1771	L	1764	1764	A_1	1771
$^7F_2$	—	1345	L*	—	1339	L*	1133	1127	A_2	1340
(5)	—	1288	L*	1268	1264	L*	1127	1224	B_1	1267
	—	1224	L*	1185	1190	L*	1089	1083	B_2	1183–1199
	947	950	R/L	938	941	L	945	942	A_1	939
	890	881	R/L	883	870	L	876	869	A_1	869–846
$^7F_1$	404	398	R/L	380	393	L	379	393	A_2	
(3)	358	357	R/L	351	362	L	353	367	B_2	
	—	—	R/L	330	341	L	328	335	B_1	
$^7F_0$	0	0	R/L	0	0	L	1	1	A_1	

In Eu_2BaZnO_5 crystals, the local symmetry of Eu^{3+} ions is C_s. For this symmetry, all B_q^k and S_q^k with even k and q values have non-vanishing values, thus the CF Hamiltonian has 15 CF parameters.

Because of the limited set of experimentally found energy levels and in order to reduce the number of parameters, we adopt the following restrictions:

(1) To obtain an adequate estimation of the spin–orbit parameter, ζ, that characterizes the position of J states inside the LS multiplet, we have used a seven parameter free ion Hamiltonian including the Racah electrostatic parameters (E_1, E_2, E_3), three configuration interaction parameters (α, β, γ) and the spin–orbit parameter ζ.

(2) We use the C_{2v} symmetry for the Eu^{3+} ion. In this symmetry the CF parameters are reduced to nine (all imaginary parameters vanish).

In C_s symmetry, the selection of a standard set of parameters (in order to compare resulting CF parameters with those obtained in other systems) suffers from several problems mainly due to the fact that there is no principal symmetry axis, so that the quantization z-axis can be arbitrarily selected. Thus, apparently different sets of starting CF parameters (from which we must obtain identical CF splitting) can be used and the relations between these different sets are not clearly established [17]. In contrast, in the approximated C_{2v} symmetry (this means to select the z-axis in a special direction coincident with a nearly C_2 axis), once an initial set of parameters is established, other equivalent sets can be obtained by standard transformations [18].

As observed in figure 2, both europium ions are surrounded by three oxygen ions forming a Y figure and other four oxygen ions are in a rhombohedral configuration in the perpendicular plane. The nearly C_2 axis is parallel to the bonds Eu(1, 2)–O(3), i.e. parallel to x and z respectively for Eu(1) and Eu(2). The distortion of these four ions from a rectangle is higher at the Eu(1) site, so the Eu(2) site is closer to a C_{2v} symmetry (bottom part of the figure).

Initial CF parameters have been obtained by point charge electrostatic calculation through standard lattice sum computations using the structural data reported [2]. Because the two Eu sites do not have the same principal nearly C_2 axis, several choices of z-axis are possible. Once the nearly C_2 axis is determined, we have selected the orientation of the orthogonal system that gives a positive value of B_2^0 parameter for each Eu site. To perform the calculations, all free ion parameters (except the spin–orbit parameter and the average energy of the 4f configuration) are fixed to standard values [19]: $E_1 = 5510.0\ \mathrm{cm}^{-1}$, $E_2 = 24.22\ \mathrm{cm}^{-1}$, $E_3 = 528.0\ \mathrm{cm}^{-1}$, $\alpha = 20.0\ \mathrm{cm}^{-1}$, $\beta = -640.0\ \mathrm{cm}^{-1}$, $\gamma = 1750.0\ \mathrm{cm}^{-1}$. With these restrictions, the spectra were fitted with standard methods to a C_{2v} Hamiltonian. The truncated matrix used in this calculation for $^5\mathrm{D} + {}^7\mathrm{F}$ multiplets includes full J mixing.

Accurate fitting was obtained when the highest three levels of $^7F_2$ multiplet (which forms a broad structure around 1200–1300 cm^{-1} above the ground state) were ruled out of the calculations. The observed peaks are shifted about 100 cm^{-1} and the splitting is considerably larger (150 cm^{-1}) than the calculated one (40 cm^{-1}). Moreover the width of these peaks (figures 4 and 5) is irregularly large; at 50 K it is about ten times that of the other peaks. These characteristics seem to indicate that the three upper levels of the $^7F_2$ multiplet are perturbed in some way.

Crystal field parameters obtained for both Eu sites are reported in table 3. Both sets of parameters are very similar having low axial (B_2^0) and orthorhombic (B_2^2) parameters, large values of fourth-rank parameters and medium values of sixth-rank parameters. Low values of B_2^0 and B_2^2 parameters are due to the experimentally obtained small $^7F_1$ and $^5D_1$ splitting. Large values of fourth-rank parameters are characteristic of compounds with O ions as ligands for rare earth ions and are related to the covalence of oxygen bonds. Fourth- and sixth-rank parameters are sensitive to overlap and covalent effects in the chemical bonds giving large values of these parameters [20, 21]. The similarity of both sets of CF parameters was expected, given the resemblance in the environments and bond distances of the Eu ions. In [5], where europium dopes the crystalline matrix Y_2BaZnO_5, the CF parameters for both Eu sites are quite different probably due to the different environments of the Eu ions which occupy yttrium sites in the matrix.

The obtained spin–orbit coupling value $\zeta = 1280(70)\ \mathrm{cm}^{-1}$ is similar to those in other paramagnetic Eu oxides. The large error is related to the restrictions in the calculations. To compare this value with the reported value ($\lambda = 365\ \mathrm{cm}^{-1}$) obtained by magnetic

Table 3. Crystal field parameters (in cm^{-1}) for the two Eu^{3+} sites in Eu_2BaZnO_5. Free ion parameters used to perform the calculations are: $E_1 = 5510.0$ cm^{-1}, $E_2 = 24.22$ cm^{-1}, $E_3 = 528.0$ cm^{-1}, $\alpha = 20.0$ cm^{-1}, $\beta = -640.0$ cm^{-1} and $\gamma = 2750.0$ cm^{-1}.

	Site 1	Site 2
B_2^0	122 ± 15	133 ± 15
B_2^2	25 ± 9	39 ± 9
B_4^0	1523 ± 35	1506 ± 35
B_4^2	-74 ± 33	-57 ± 32
B_4^4	1312 ± 25	1320 ± 25
B_6^0	-493 ± 41	-476 ± 41
B_6^2	429 ± 40	484 ± 38
B_6^4	-295 ± 29	-257 ± 29
B_6^6	-27 ± 38	-114 ± 37

measurements in the same compound [12], we need to note that the definition of spin–orbit parameter, λ, used in the work of Goya *et al* is related to the standard definition used in these calculations as:

$$\zeta A(LS) = \lambda$$

with $A(LS)$ a characteristic constant for a given $|LS\rangle$ multiplet [22]. Our spin–orbit value corresponds to a value of $\lambda = 304(16)$ cm^{-1}, that is lower than the value of Goya *et al* but is in good agreement with the Eu_2CuO_4 value ($\lambda = 303$ cm^{-1}) [23].

6. Excitation energy and temperature effects

Several features observed in the dependence of the spectra of Eu_2BaZnO_5 on the temperature and the excitation energy reveal the complexity of the processes where electronic transitions are involved. As temperature decreases from 300 K to 35 K, the following are observed:

(i) The intensity of the RCF peaks increases independently of the excitation energy.

(ii) In off-resonance condition, the intensity of the luminescence peaks decreases always but the rate depends on the excitation energy.

(iii) The intensity of the peaks related to transitions from the $^5D_0$ level decreases about three times faster than those from the $^5D_1$ level for 514.5 nm excitation.

(iv) Absorption peaks corresponding to $^7F_0 \rightarrow {}^5D_{0,1,2}$ and $^7F_1 \rightarrow {}^5D_1$ transitions are observed in the emission spectra. Some are observed at 300 K down to low temperature and others change from emission to absorption peaks such as the $^7F_0 \rightarrow {}^5D_0$ transition (figure 6).

(v) Anti-Stokes luminescence peaks (at energies up to 3100 cm^{-1} above the excitation energy) are observed down to $T \approx 150$ K.

(vi) Three peaks of the $^5D_0 \rightarrow {}^7F_2$ transition are much wider than expected even at 35 K (FWHM $\sim$ 10 times the other peaks).

Some of these features can be understood but others are still unclear:

(i) The intensity of the RCF transitions increases when temperature is lowered (figure 4). Because the intensity of an absorption process is proportional to the population of the initial state, the increase of the RCF transitions should be explained by the increase of the ground state population when temperature decreases. Nevertheless, the evolution of the experimental integrated intensity of the RCF transitions versus temperature is qualitatively different to that of the ground state population ($^7F_0$), showing a deviation of around 20% in the range between RT and 170 K and a very large one in the low temperature range. This

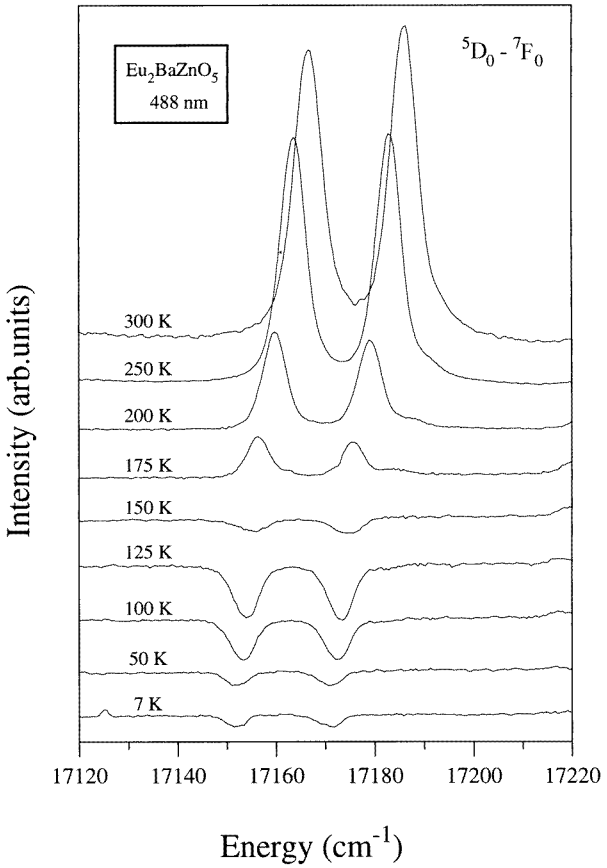

Figure 6. Evolution of the $^5D_0 \rightarrow {}^7F_0$ transition with temperature. In the emission spectra, luminescence peaks are observed as absorption ones at temperatures below 160 K.

is in opposition to what happens in Nd_2BaZnO_5 [11] where the RCF transition intensity follows well the ground state population.

(ii) In the off-resonance condition for the excitation, the thermal population of the lowest multiplets ($^7F_1$ and $^7F_2$) and/or the thermal population of phonons are fundamental to achieve the excitation of one electron to the ^5D levels, specially at high temperatures. Therefore, as the temperature decreases the emission is expected to decrease depending on the difference between the incident photon energy and that of some ^5D level, as observed.

(iii) On the other hand, figure 5 shows that when temperature is lowered, the decrease of the intensity of the peaks related to transitions from $^5D_0$ is much quicker than that for transitions from $^5D_1$ for both excitation energies (488 and 514.5 nm). This behaviour can be explained by the temperature dependence of the non-radiative rate [24]: for transitions between $4f^n$ levels, this probability is given by:

$$N(T) \propto (1+n)^p$$

where $p = E_i - E_j/\hbar\omega$ and ω is a phonon frequency. The only dependence on temperature is in $n(\omega, T) = [\exp(\hbar\omega/kT) - 1)]^{-1}$. In the present case, the energy difference between $^5D_0$ and $^5D_1$ levels is around 1700 cm^{-1}. Quantitatively, the observed behaviour can be explained considering that phonons of about 340 cm^{-1} are the ones involved in this process.

In principle all phonons can participate in the process, depending on their electron–phonon coupling. Therefore, the obtained value of 340 cm^{-1} is an indication of the mean phonon value for this process. Note that this corresponds to the mean value of the phonon energy distribution (figure 1). This is in contrast with the usual selection of the more energetic phonon in the non-radiative processes. At room temperature, this multiphonon non-radiative decay to the $^5D_0$ singlet is very probable and the emission takes place from this level. In contrast, at low temperature the non-radiative decay probability decreases and the luminescence process starts mainly at the $^5D_1$ triplet.

(iv) In a certain range of temperatures the reabsorption process (to the $^5D_0$ level and specially to the $^5D_1$ triplet) becomes important and is, in fact, a path for the selective population of the $^5D_1$ multiplet.

(v) Figure 7 exhibits luminescence measurements where the excitation wavelength is 633 nm (15 803 cm^{-1}). We are again in off-resonance condition, but now the excitation energy is far below (about 1380 cm^{-1}) the $^5D_0$ (17 183 cm^{-1}) singlet. Nevertheless, luminescence peaks coming from this level to all ^7F multiplets are observed, some of them ($^5D_0 \rightarrow {}^7F_0$, $^7F_1$, $^7F_2$) at frequencies higher than the excitation one. The abscissa axis shows the Raman shift from the laser wavelength. Note that even transitions from the $^5D_1$ (18 934 cm^{-1}) multiplet (more than 3100 cm^{-1} above the excitation energy) are detected as weak peaks at RT (dots in figure 7). This attribution of high (low) intensity peaks to transitions from $^5D_0$ ($^5D_1$) is in agreement with the assignment made in figure 5. When temperature is lowered, the integrated intensity of the phonon peaks remains almost unchanged while luminescence intensity decreases drastically.

The up-conversion process cannot be possible since it requires a first transition to a level that, in our case, does not exist. On the other hand, a double photon excitation is disregarded because the luminescence intensity is observed to vary linearly with the incident power instead of an expected quadratic dependence for second-order processes. The most probable explanation is the following: because the energy difference between the $^7F_2$ higher levels and the $^5D_0$ singlet (around 15 840 cm^{-1}) corresponds very well with the excitation energy 633 nm, the excitation process could lie in exciting electrons from these thermally populated $^7F_2$ levels to the $^5D_0$ level. This process is possible whenever the temperature is high enough to have an appreciable population in the $^7F_2$ levels. This can be a possible explanation although the observed luminescence intensity is slightly higher than the expected one.

(vi) Finally, as can be observed in figures 4 and 5, the peaks corresponding to transitions to the three highest $^7F_2$ levels are specially broad even at low temperature, both in luminescence and Raman scattering spectra; therefore, such a broadening has to be associated with the $^7F_2$ multiplet. Furthermore, in the Eu_2BaCoO_5 oxide [9], where the Eu ion occupies only one C_{2v} symmetry site, the $^5D_0 \rightarrow {}^7F_2$ transition presents the three highest $^7F_2$ levels as narrow peaks, not as a band, while the Eu^{3+}:Y_2BaZnO_5 compound [5], with *Pnma* structure and Eu ions in two C_s sites, shows these peaks also as broad bands and shifted with respect to calculated values. For these reasons, the width seems to be associated with the *Pnma* structure. In particular it may be due to a hybridization of these Eu levels with other levels or bands, for example, with orbitals of the oxygen ions which are very close to the europium ion. The large values of the obtained fourth-rank CF parameters, that are related to the covalence, support this hypothesis.

7. Conclusions

Reflectance, Raman and luminescence experiments have been performed on the Eu_2BaZnO_5 compound. In reflectance measurements, the transitions from ^7F_J ($J = 0, 1, 2$) to ^5D_J

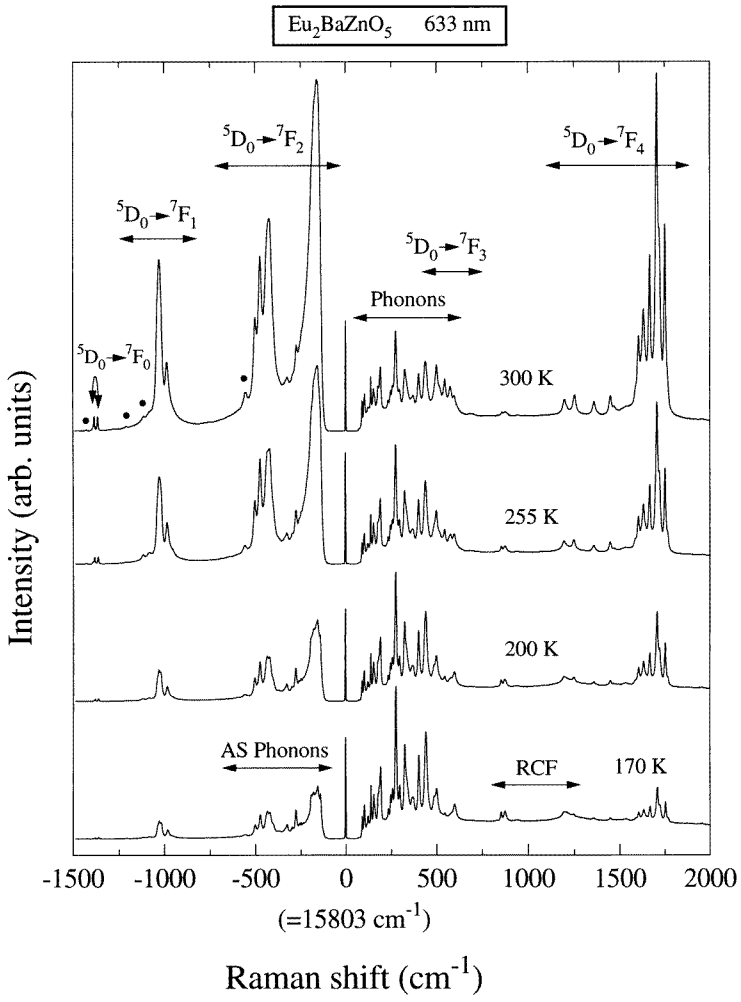

Figure 7. Raman spectra at different temperatures using a 633 nm excitation energy. In addition to Stokes and anti-Stokes Raman phonons, Raman crystal field transitions and luminescence (labelled as $^5D_0 \rightarrow {}^7F_J$) are observed. Dots indicate the weak $^5D_1 \rightarrow {}^7F_J$ transitions.

($J = 0, 1, 2$) multiplets have been identified, and the energy of the involved levels determined. Raman and luminescence experiments have been performed at room and low temperature with three different excitation energies always in off-resonance condition. In addition to Raman phonons, Raman CF transitions between ground state and $^7F_2$, $^7F_3$ and $^7F_4$ multiplets have been identified in the Raman spectra, and the ^5D_J ($J = 0, 1$) $\rightarrow$ ^7F_J ($J = 0$ to 4) transitions have been labelled in luminescence spectra. By combining the three spectroscopic techniques, almost all electronic levels of $^7F_{0,1,2,3,4}$ and $^5D_{0,1,2}$ multiplets are obtained for both Eu sites, the maximum energy difference between equivalent levels being 20 cm^{-1}. Crystal field parameters have been calculated and have come out to be very similar for both Eu^{3+} sets. The approximation from C_s to C_{2v} symmetry is reasonable considering the good fit of the observed levels. The obtained large values of fourth-rank parameters have been found to be related to the covalence of Eu–O bonds. The evolution of the experimental integrated intensity of the RCF transitions versus temperature differs

qualitatively from that of the ground state population ($N_{^7F_0}$), showing a deviation of around 20% in the high temperature range and a much higher one in the low temperature range. The variation of the relative intensity of the luminescence peaks associated to transitions from $^5D_0$ and $^5D_1$ levels as a function of temperature is related to the dependence of the multiphonon non-radiative decay on temperature. Luminescence spectra obtained using the 633 nm excitation energy, far below the $^5D_0$ level, show transitions from this level. The intensity of these transitions is slightly higher than expected considering that the excitation process starts at the thermally populated $^7F_2$ excited multiplet. The peaks corresponding to transitions to the three highest $^7F_2$ levels are specially broad even at low temperature, indicating that they are perturbed probably due to a hybridization with other levels of the crystal. The appearance of absorption peaks in the luminescence spectrum suggests that reabsorption processes are occurring.

Acknowledgments

We thank Dr J García-Solé for valuable discussions. We acknowledge financial support from the C.I.C.yT. (Spanish Ministerio de Educacion y Ciencia) under contracts MAT 95-2042-E, MAT 96-0395-CP and MAT 97-0725 and from the 'Fundación Domingo-Martínez'. ST has been supported by the Comunidad Autonoma de Madrid under contract No AE00147/95.

References

[1] Michel C and Raveau B 1983 *J. Solid State Chem.* **49** 150
[2] Taibi M, Aride J, Darriet J and Boukhari A 1991 *J. Less-Common Met.* **169** 217
[3] Kaminskii A A 1975 *Laser Crystals (Springer Series in Optical Sciences 14)* (Berlin: Springer)
[4] Arizmendi L and Cabrera J M 1985 *Phys. Rev.* B **31** 7138
[5] Taibi M, Aride J, Antic-Fidancev E, Lemaitre-Blaise M and Porcher P 1989 *Phys. Status Solidi* a **115** 523
[6] Malta O L, Antic-Fidancev E, Lemaitre-Blaise M, Milicic-Tang A and Taibi M 1995 *J. Alloys Compounds* **228** 41
[7] Hölsä J and Leskelä M 1985 *Mol. Phys.* **54** 657
[8] Taibi M, Antic-Fidancev E, Aride J, Lemaitre-Blaise M and Porcher P 1993 *J. Phys.: Condens. Matter* **5** 5201
[9] Taboada S, de Andrés A, Muñoz-Santiuste J E, Prieto C, Martínez J L and Criado A 1994 *Phys. Rev.* B **50** 9157
[10] Strach T, Ruf T, Cardona M, Lin C T, Jandl S, Nekvasil V, Zhigunov D I, Barilo S N and Shiryaev S V 1996 *Phys. Rev.* B **54** 4276
[11] de Andrés A, Taboada S, Martínez J L, Dietrich M, Litvinchuk A and Thomsen C 1997 *Phys. Rev.* B **55** 3568
[12] Goya G F, Mercader R C, Causa M T and Tovar M 1996 *J. Phys.: Condens. Matter* **8** 8607
[13] de Andrés A, Taboada S, Martínez J L, Salinas A, Hernández J and Sáez-Puche R 1993 *Phys. Rev.* B **47** 14 898
[14] Ofelt G S 1963 *J. Chem. Phys.* **38** 2171
[15] Koster G F, Dimmoch J O, Wheeler R G and Statz H 1965 *Properties of the Thirty-two Point Groups* (Cambridge, MA: MIT)
[16] Lempicki A, Samelson H and Brecher C 1968 *J. Mol. Spectrosc.* **27** 375
[17] Rudowicz C 1986 *J. Chem. Phys.* **84** 5045
[18] Rudowicz C 1985 *J. Chem. Phys.* **83** 5192
[19] Huang J, Loriers J, Porcher P, Teste de Sagey G, Caro P and Levi-Clements C 1984 *J. Chem. Phys.* **80** 6204
[20] Antic-Fidancev E, Lemaitre-Blaise M and Caro P 1987 *New J. Chem.* **11** 467
[21] Newman D J 1978 *Aust. J. Phys.* **31** 79
[22] Wybourne B G 1965 *Spectroscopic Properties of Rare Earths* (New York: Wiley–Interscience)
[23] Tovar M, Rao D, Barnett J, Oseroff S, Thompson J D, Cheong S-W, Fisk Z, Vier D C and Schultz S 1989 *Phys. Rev.* B **39** 2661
[24] Blasse G 1993 *Solid State Luminescence: Theory, Materials and Devices* ed A H Kitai (London: Chapman and Hall) pp 33–34